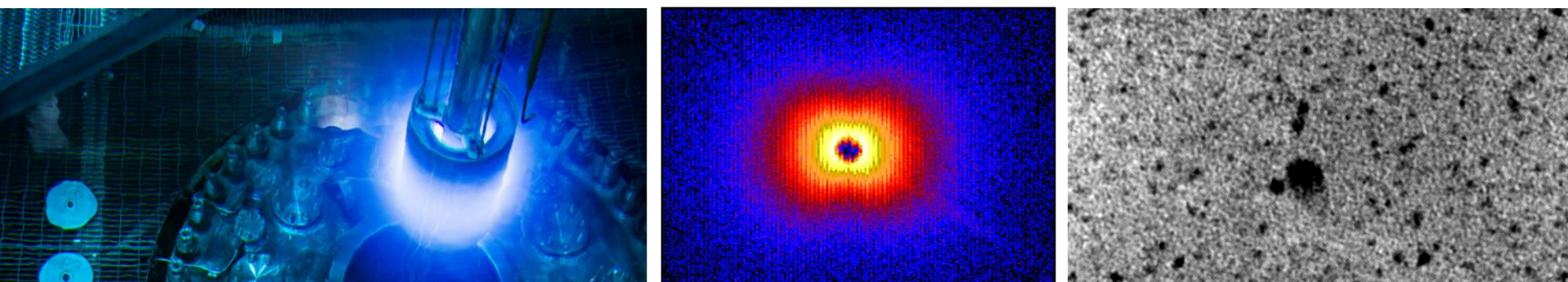


Exceptional service in the national interest



Microstructural stability of irradiated FeCrAl alloys for fuel cladding applications

Presented by:

Samuel A. Briggs¹



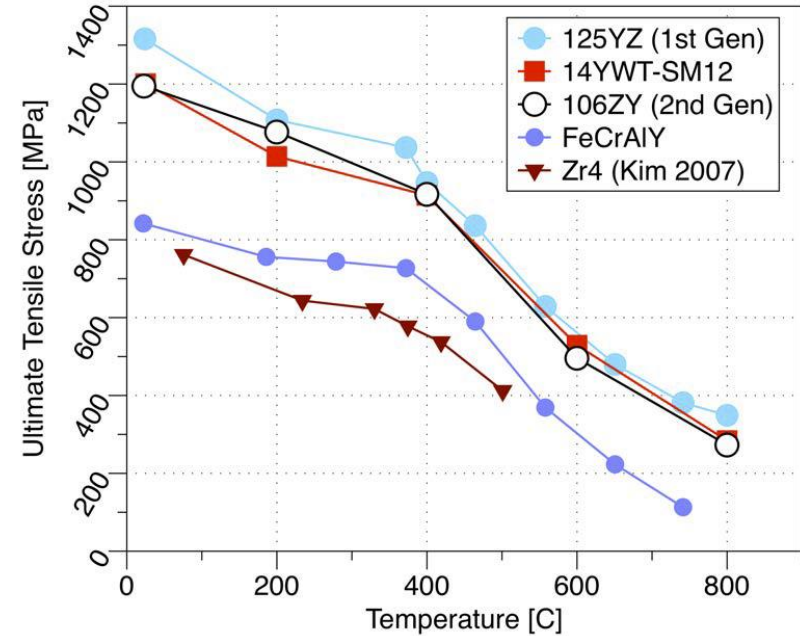
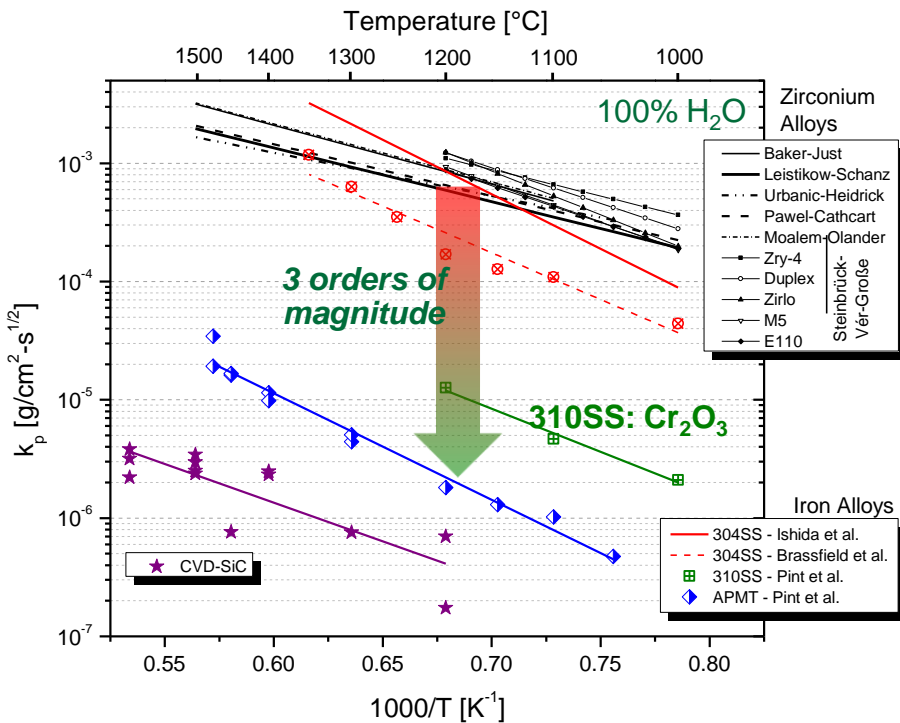
Co-authors: D. Zhang², K.G. Field², K.C. Littrell², D.T. Hoelzer², S.N. Dryepondt², P.D. Edmondson², K. Hattar¹

¹Sandia National Laboratories, ²Oak Ridge National Laboratory



Sandia National Laboratories is a multimission laboratory managed and operated by National Technology and Engineering Solutions of Sandia, LLC, a wholly owned subsidiary of Honeywell International, Inc., for the U.S. Department of Energy's National Nuclear Security Administration under contract DE-NA0003525.

ODS FeCrAl Alloy Development for Nuclear Applications



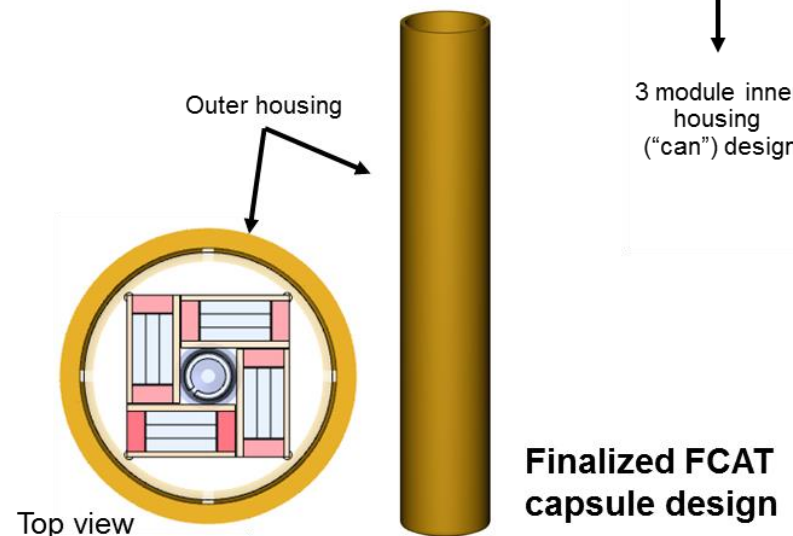
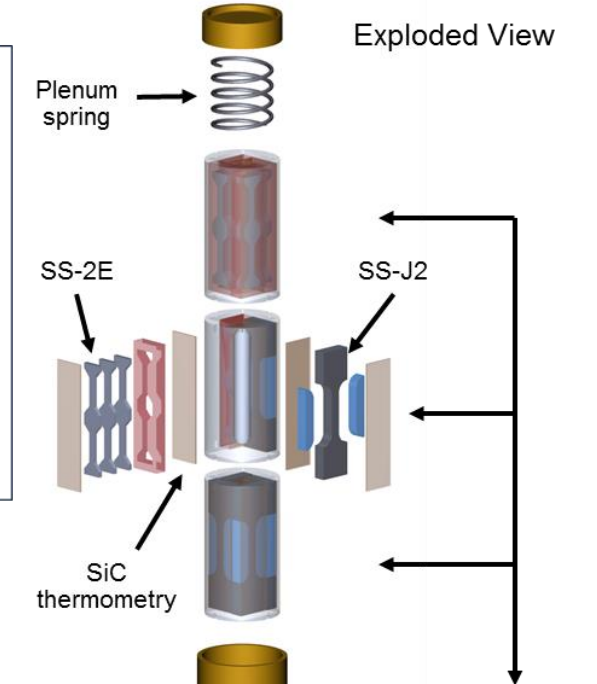
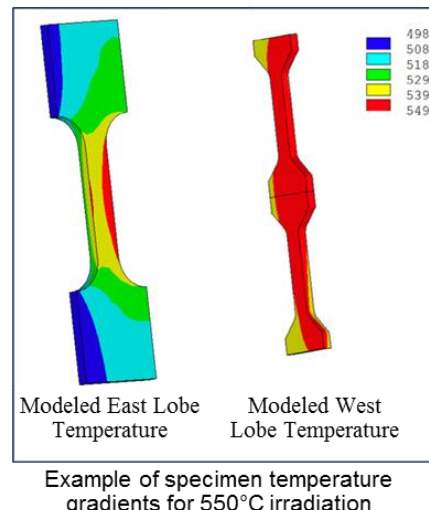
- Exhibit high strength at elevated temperatures, excellent oxidation and corrosion resistance, high thermal conductivity, low thermal expansion and good void swelling resistance
- Nanoparticles could lead to high irradiation resistance due to a higher density of defect sinks compared to wrought FeCrAl alloys

FCAY and FCAT Rabbits

PURPOSE: rapid screening of alloy irradiated tensile properties and microstructure

Specifications:

- SS-J2 and SS-2E flat sheet tensile specimen geometries
 - Design temperatures of 200-550 °C
- Temperature monitored passively using SiC thermometry
- Modular; can accept any ratio of SS-J2 to SS-2E specimen configurations
- Robust, proven design over the past 4+ years



FCAY and FCAT Rabbits

PURPOSE: rapid screening of alloy irradiated tensile properties and microstructure

Specifications:

- SS-J2 and SS-2E flat sheet tensile specimen geometries
 - Design temperatures of 200-550 °C
- Temperature monitored passively using SiC thermometry
- Modular; can accept any ratio of SS-J2 to SS-2E specimen configurations
- Robust, proven design over the past 4+ years



FCAY and FCAT Rabbits

Alloys studied:

1. Model alloys (M): F1C5AY, B125Y, B154Y-2, B183Y-2
2. Engineering grade alloys (E): C06M, C35M, C36M, C37M, C35MN, C35M10TC
3. Commercial alloys (C): Kanthal APMT™, and Alkrothal 720
4. ODS Alloys (O): 125YF

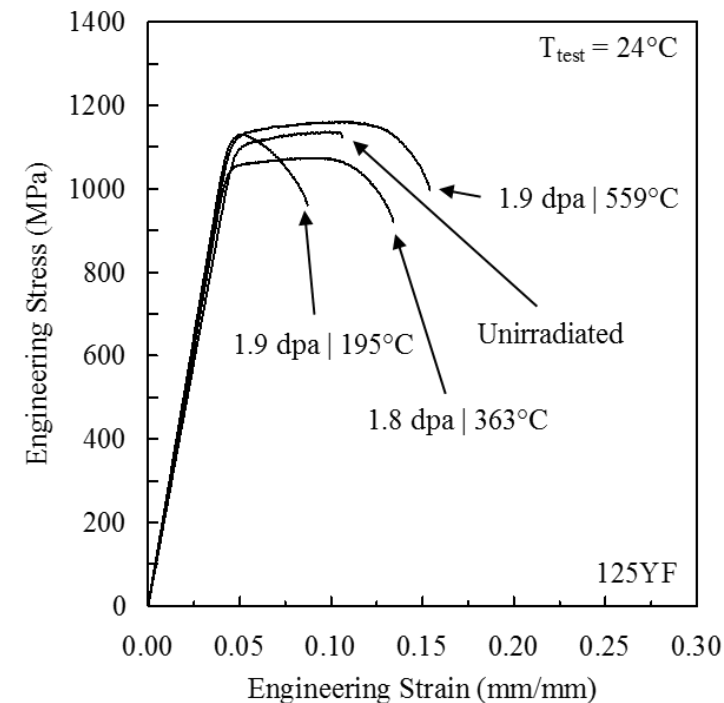
Capsule ID	Number Samples	Alloys	Exposure Time (hrs)	Neutron Flux (n/cm ² s) E > 0.1 MeV	Neutron Fluence (n/cm ²) E > 0.1 MeV	Dose Rate (dpa/s)	Dose (dpa)	Irradiation Temperature (°C)
FCAY-01	36	M+C	120	8.54×10^{14}	3.69×10^{20}	7.7×10^{-7}	0.3	334.5 ± 0.6
FCAY-02	36	M+C	301	8.54×10^{14}	9.25×10^{20}	7.7×10^{-7}	0.8	355.1 ± 3.4
FCAY-03	36	M+C	614	8.84×10^{14}	1.95×10^{21}	8.1×10^{-7}	1.8	381.9 ± 5.4
FCAY-04	36	M+C	2456	8.74×10^{14}	7.73×10^{21}	7.9×10^{-7}	7.0	319.9 ± 10.2
FCAY-05	36	M+C	4914	8.74×10^{14}	1.55×10^{22}	7.8×10^{-7}	13.8	340.5 ± 25.7
FCAT-01	45	E+O	548	1.10×10^{15}	2.17×10^{21}	9.6×10^{-7}	1.9	194.5 ± 37.9
FCAT-02	45	E+O	548	1.04×10^{15}	2.05×10^{21}	9.1×10^{-7}	1.8	362.7 ± 21.2
FCAT-03	45	E+O	548	1.10×10^{15}	2.17×10^{21}	9.6×10^{-7}	1.9	559.4 ± 28.1
FCAT-04	45	E+O	1754	1.10×10^{15}	9.32×10^{21}	9.6×10^{-7}	8.3	200*
FCAT-05	45	E+O	1754	1.04×10^{15}	8.81×10^{21}	9.1×10^{-7}	7.9	330*
FCAT-06	45	E+O	1754	1.10×10^{15}	9.32×10^{21}	9.6×10^{-7}	8.3	550*
FCAT-07	45	E+O	4032	1.10×10^{15}	$1.82 \times 10^{22*}$	9.6×10^{-7}	16.3*	200*
FCAT-08	45	E+O	4032	1.04×10^{15}	$1.73 \times 10^{22*}$	9.1×10^{-7}	15.4*	330*
FCAT-09	45	E+O	4032	1.10×10^{15}	$1.82 \times 10^{22*}$	9.6×10^{-7}	16.3*	550*

*Target values

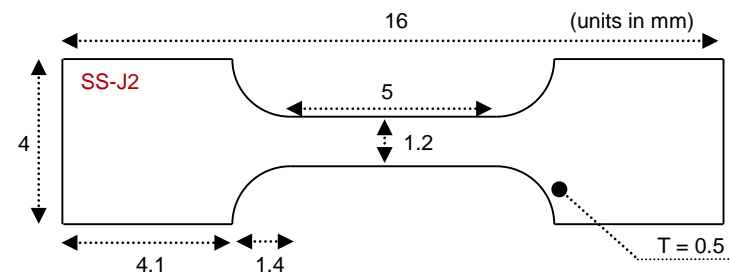
ODS FeCrAl Mechanical Properties at ~ 2 dpa

- Tensile tests performed in ambient air
- Medium to elevated temperature irradiations show little change in mechanical properties

Specimen	Irradiation Temperature (°C)	Yield Strength (MPa)	Ultimate Tensile Strength (MPa)	Uniform Elongation (%)	Total Elongation (%)
OD34	-	1085	1137	4.8	5.8
OD01	195	1108	1130	0.8	5.0
OD03	363	1037	1074	5.0	9.7
OD06	559	1104	1160	6.2	11.2



- Low temperature irradiation showed embrittlement
 - Due to cluster stability even at low dose?



Characterization techniques for nanoparticles

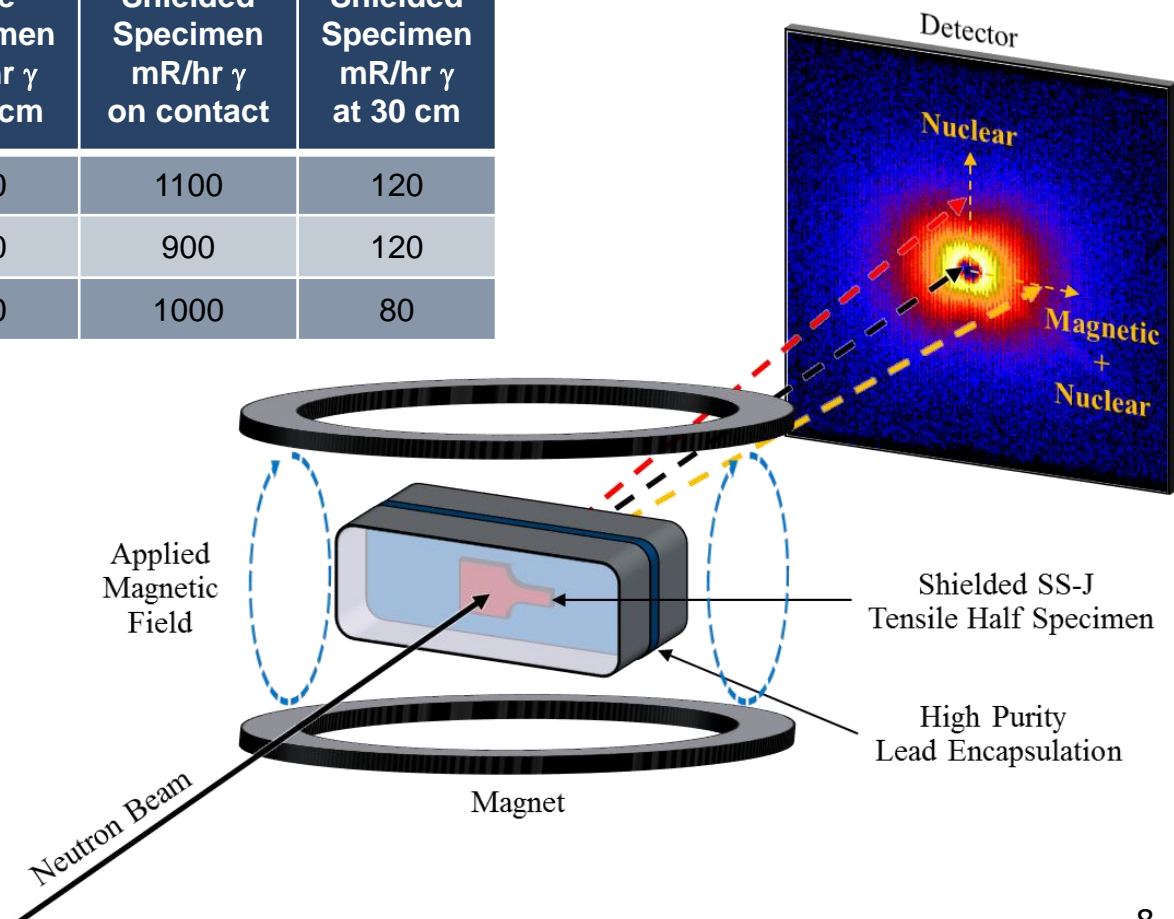
	Advantages	Disadvantages
Energy Filtered TEM (EFTEM)	<ul style="list-style-type: none">• Reveals microstructural heterogeneities• Quick/easy to perform• Direct microstructure observation	<ul style="list-style-type: none">• Poor signal to noise ratio; can limit resolution• Moderate volume analyzed• Highly dependent on sample quality• Limited composition information
Small Angle Neutron Scattering (SANS)	<ul style="list-style-type: none">• Large sampling volume; excellent counting statistics• Limited to no sample prep• Quick/easy to perform• Composition can be inferred (magnetic SANS only)	<ul style="list-style-type: none">• Indirect microstructure observation• No microstructural relationships (i.e. assumes homogenous distributions)• Requires bulk sample; increased radioactivity
Atom Probe Tomography (APT)	<ul style="list-style-type: none">• Composition information readily available• Excellent spatial resolution• Direct microstructure observation	<ul style="list-style-type: none">• Small sample volume analyzed• Dependent on sample quality• Data interpretation can be convoluted; aberration effects• Time intensive

SANS Data Configuration

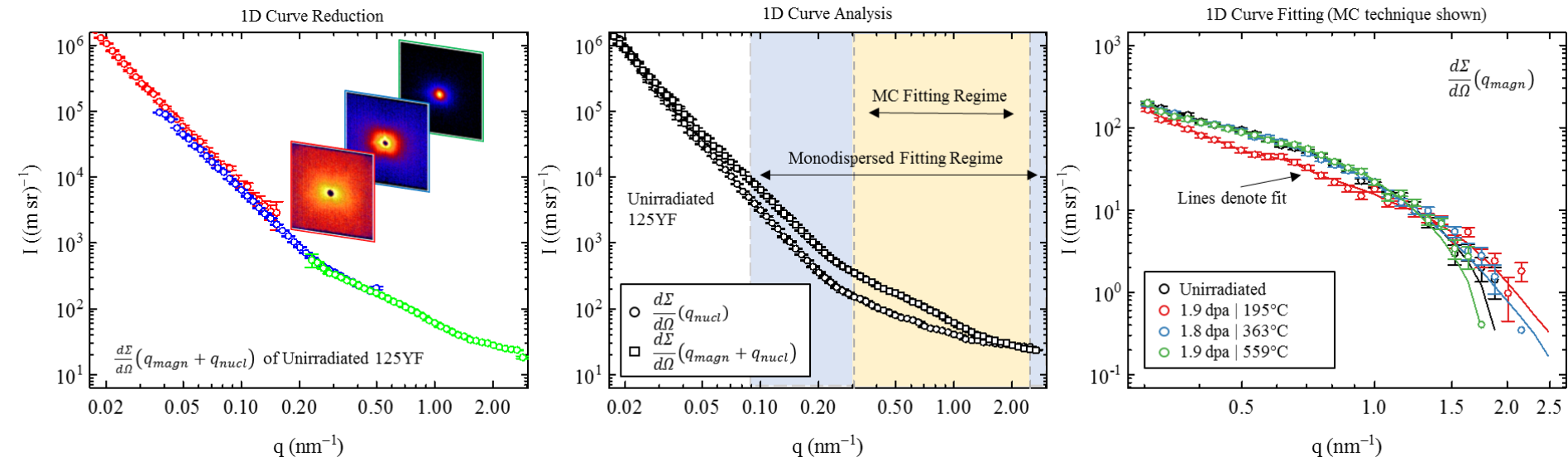
- Neutron irradiated SS-J tensile half specimens were encapsulated in Pb “piglets” to limit radioactivity while providing high quality SANS

Specimen ID	Bare Specimen mR/hr γ on contact	Bare Specimen mR/hr γ at 30 cm	Shielded Specimen mR/hr γ on contact	Shielded Specimen mR/hr γ at 30 cm
OD01	2200	160	1100	120
OD03	2000	120	900	120
OD06	1800	100	1000	80

- SANS configuration:
 - GP-SANS Line at ORNL
 - ≥ 1 T saturated magnetic field
 - 3 detector configurations: $0.00658 \leq q \text{ (nm}^{-1}\text{)} \leq 2.48$
 - Ambient air
 - 1D curves scaled to medium detector configuration



SANS Data Analysis



- Magnetic scattering contrast calculated as $1.55 \times 10^{-11} \text{ \AA}^{-4}$ using normalized Fe-Cr-Al composition¹
- A-ratios calculated assuming perfect crystals
- First order approximation of the magnetic scattering difference:

$$\frac{d\Sigma}{d\Omega}(q_{magn}) \approx \frac{d\Sigma}{d\Omega}(q_{nucl}) - \frac{d\Sigma}{d\Omega}(q_{magn} + q_{nucl})$$

- Fitting on magnetic scattering difference completed using Monte Carlo regression analysis² and monodispersed spheres³

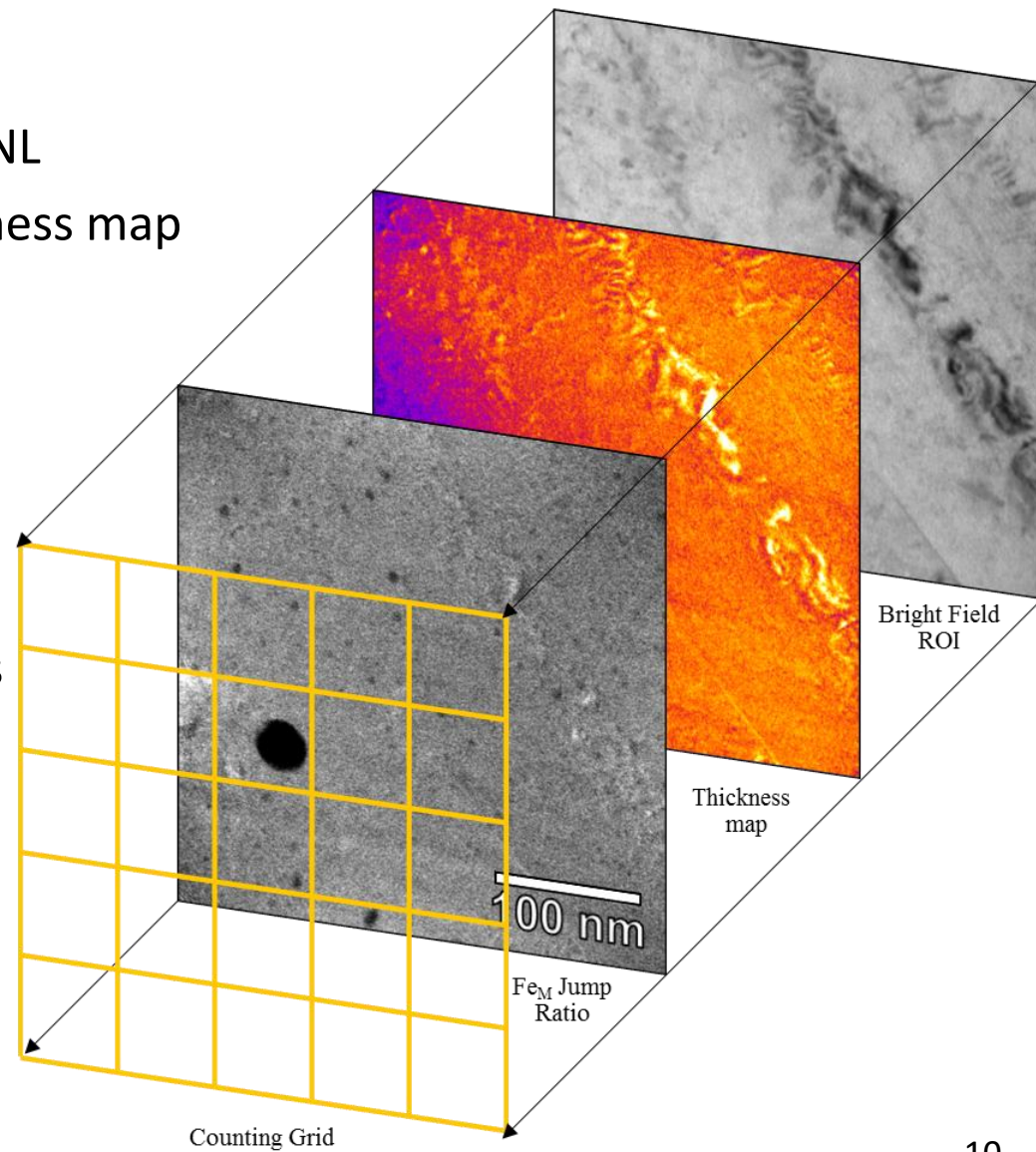
EFTEM Data Configuration and Analysis

- EFTEM Configuration:

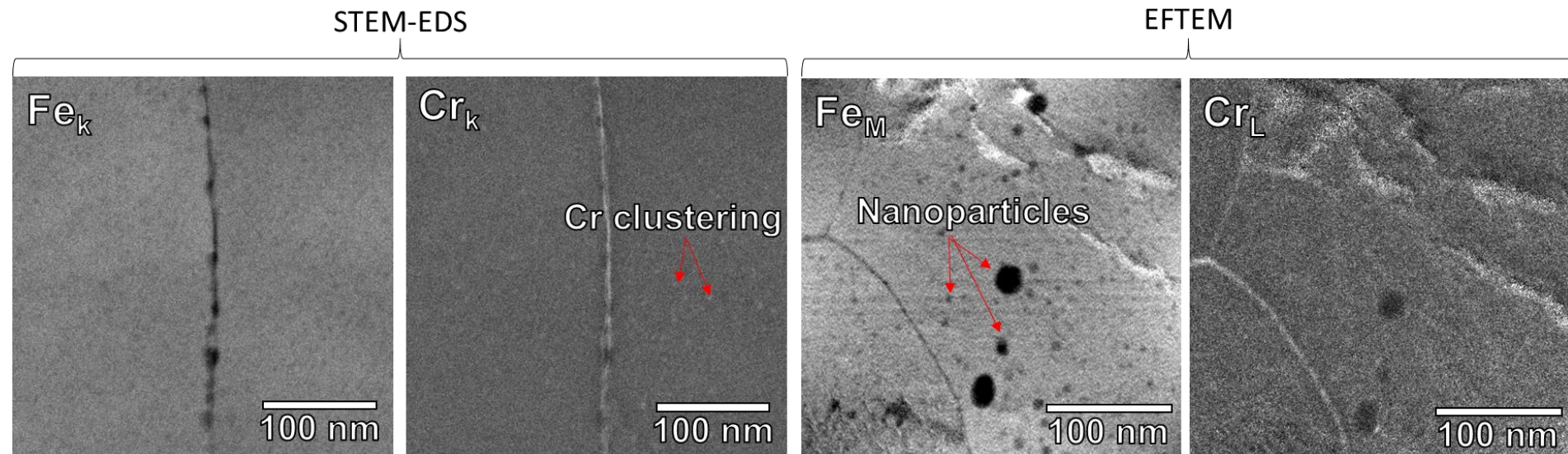
- JEOL 2100F in LAMDA at ORNL
- Fe_M jump-ratio map & thickness map per ROI
 - 10 eV slits
 - Manual drift correction
 - $\lambda = 100.41 \text{ nm}$ (calculated)

- EFTEM analysis:

- Subdivided into 25 area bins
- B/C Correction + Mean Image Filter
- Manually counted precipitates using ImageJ
- Volume calculated using avg. thickness in each bin



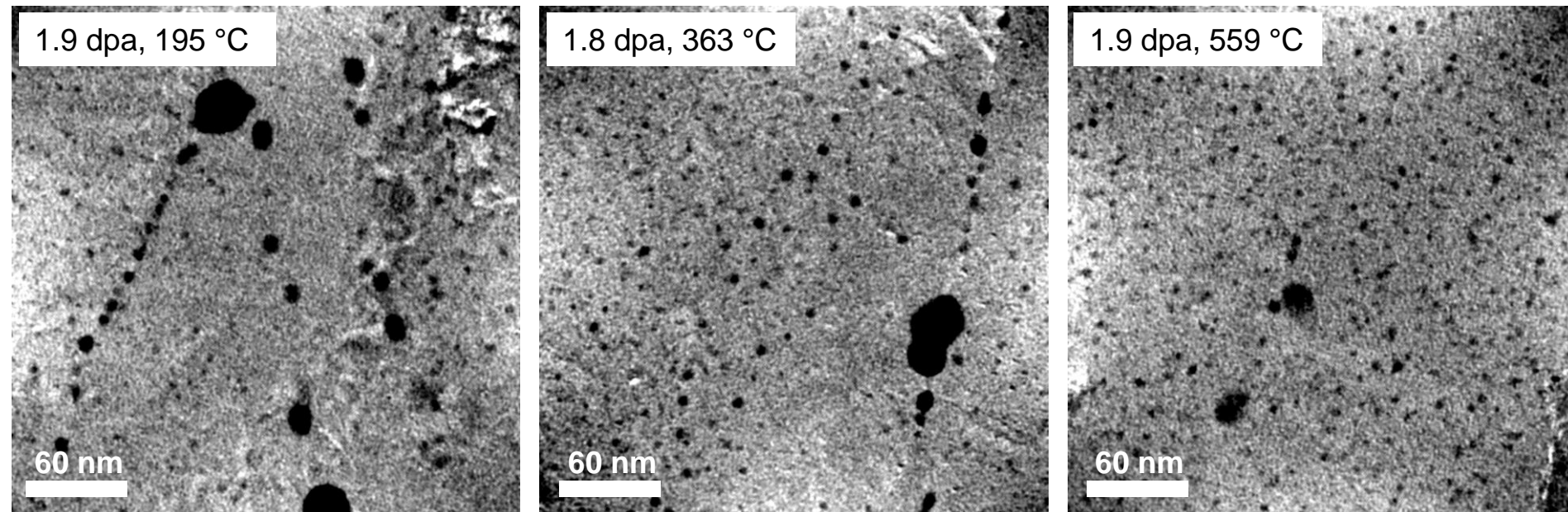
Radiation-enhanced precipitation (α')



- FeCrAl alloys have been shown to be susceptible to Cr-rich α' precipitation under neutron irradiation¹
- STEM-EDS reveals possible Cr-clustering but most likely weak composition variance to matrix
- EFTEM insensitive to detection of Cr-cluster found in STEM-EDS

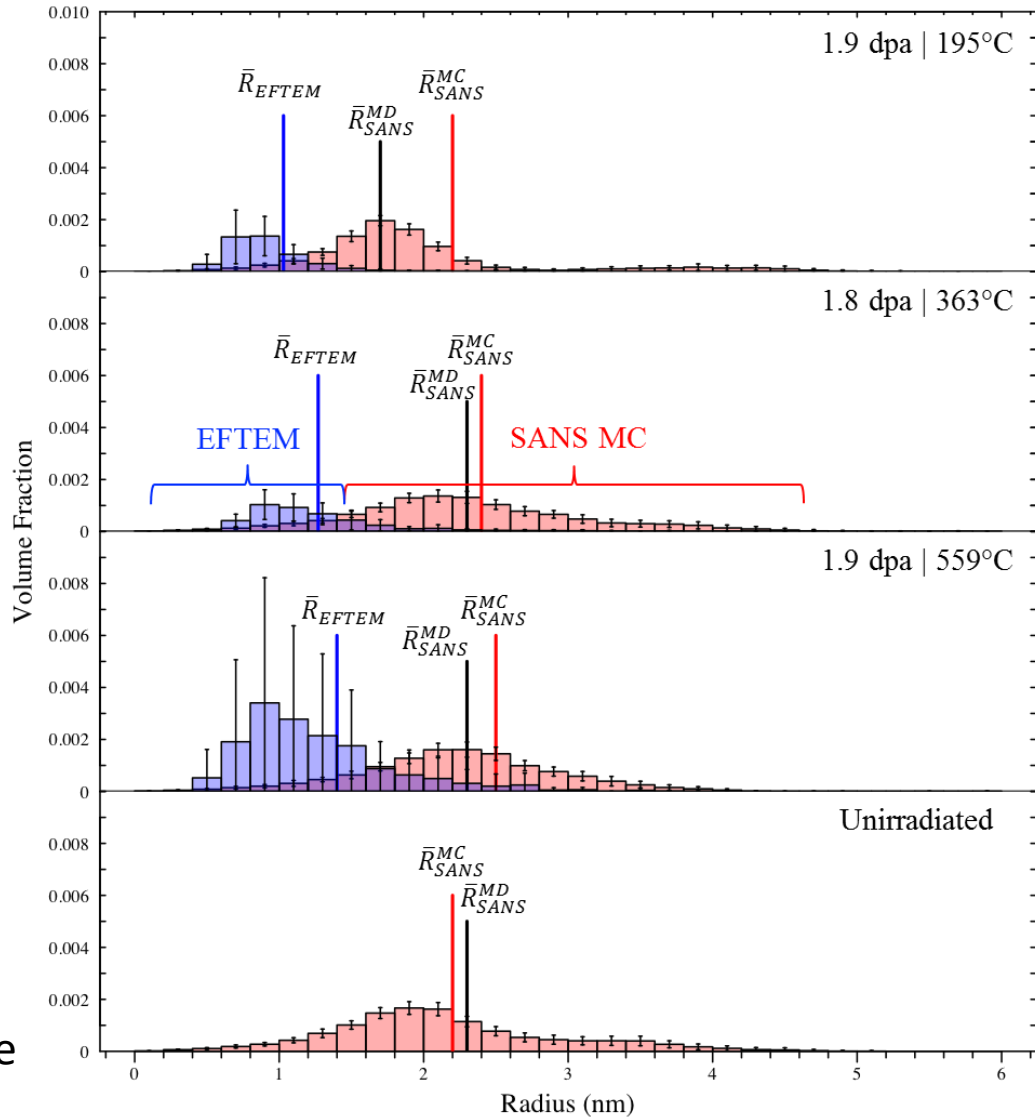
EFTEM Qualitative Observations

- Bimodal size distribution apparent
 - Larger precipitates decorate grain boundaries (likely YAG and alumina phases)
 - Finer precipitate dispersion throughout bulk material
- Heterogeneous distributions – large grain-to-grain variation



Size Distributions

- Peak shifts and distribution broadening/tailing towards larger sizes suggest:
 - 1.9 dpa | 195 °C: **NP instability**
 - 1.8 dpa | 363 °C: **NP stability**
 - 1.9 dpa | 559 °C: NP coarsening
- Difference in size distributions between SANS and EFTEM due to varying resolution limits
- Large error in EFTEM results are indicative of technique errors and grain-to-grain heterogeneity
- Reasonable agreement between the monodispersed (MD) approximation and "brute-force" Monte Carlo (MC) model mean size suggests monodispersed model is a reasonable first-order analysis



A-ratio determination (composition + structure)

Particle	ρ (g/cm ³)	$\Delta\rho_{nuclear}^2$ ($\times 10^{-12}$ Å)	$\Delta\rho_{magnetic}^2$ ($\times 10^{-12}$ Å)	Calculated A-ratio
YAG - $Y_3Al_5O_{12}$	4.56	2.73	0.16	6.68
YAP - $YAlO_3$	5.35	1.26	0.16	13.30
YAM - $Y_4Al_2O_9$	4.56	5.18	0.16	3.99
Al_2O_3	3.95	1.16	0.16	14.40
AlN	3.26	37.5	0.16	42.34
Y_2O_3	5.01	5.52	0.16	3.81
α'	7.20	0.11	0.16	2.44

Specimen ID	Irradiation Temp. (°C)	A-ratio (unitless)	
		SANS MD	SANS Monte Carlo
OD34	-	1.75 ± 0.05	2.75 ± 0.54
OD01	195	1.31 ± 0.08	2.06 ± 0.37
OD03	363	1.63 ± 0.05	2.51 ± 0.48
OD06	559	1.96 ± 0.11	2.32 ± 0.40

- Highly dependent on stoichiometry, chemical composition, and structure (density)
- A-ratio of 1.75-2.75 in the as-received condition suggests far-from perfect particle phases (amorphization, Fe/Cr substitution, etc.)
- Reduction after irradiation could be due to particles changing over the course of irradiation or the addition of the Cr-rich α' phase in OD01 and OD03

A-ratio determination (composition + structure)

Specimen ID	Irradiation Temp. (°C)	A-ratio (unitless)	
		SANS MD	SANS Monte Carlo
OD34	-	1.75±0.05	2.75±0.54
OD01	195	1.31±0.08	2.06±0.37
OD03	363	1.63±0.05	2.51±0.48
OD06	559	1.96±0.11	2.32±0.40

Contrast (ρ^2) independent

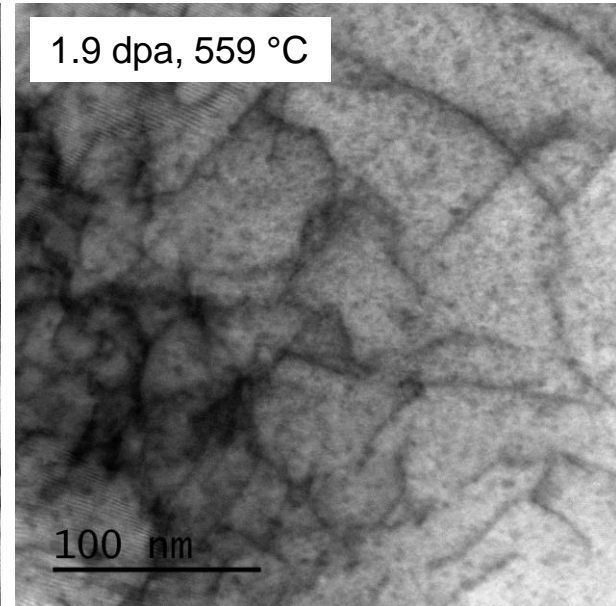
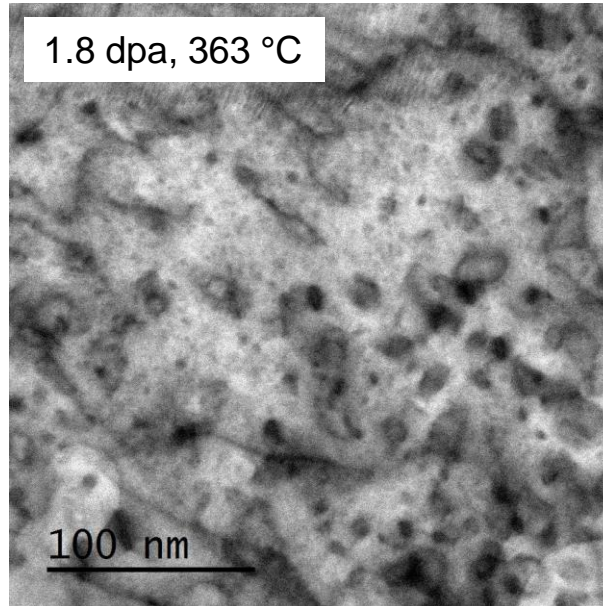
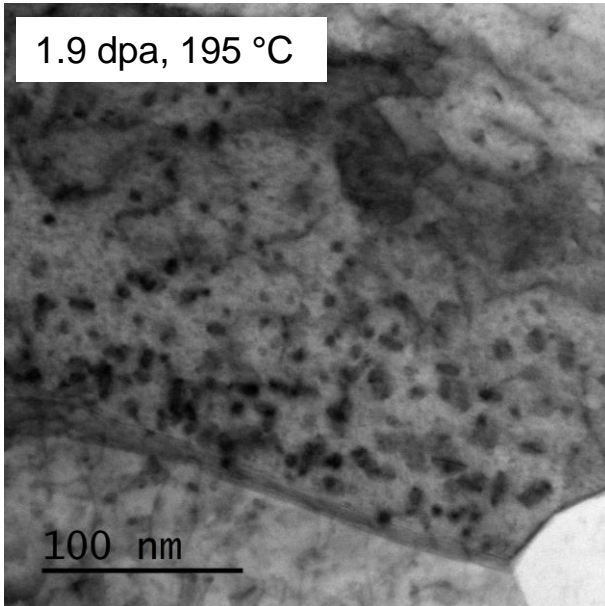
Contrast (ρ^2) used as a fitting parameter

Reduction after low temperature irradiation → instability?

- Highly dependent on stoichiometry, chemical composition, and structure (density)
- A-ratio of 1.75-2.75 in the as-received condition suggests far-from perfect particle phases (amorphization, Fe/Cr substitution, etc.)
- Reduction after irradiation could be due to particles changing over the course of irradiation or the addition of the Cr-rich α' phase in OD01 and OD03

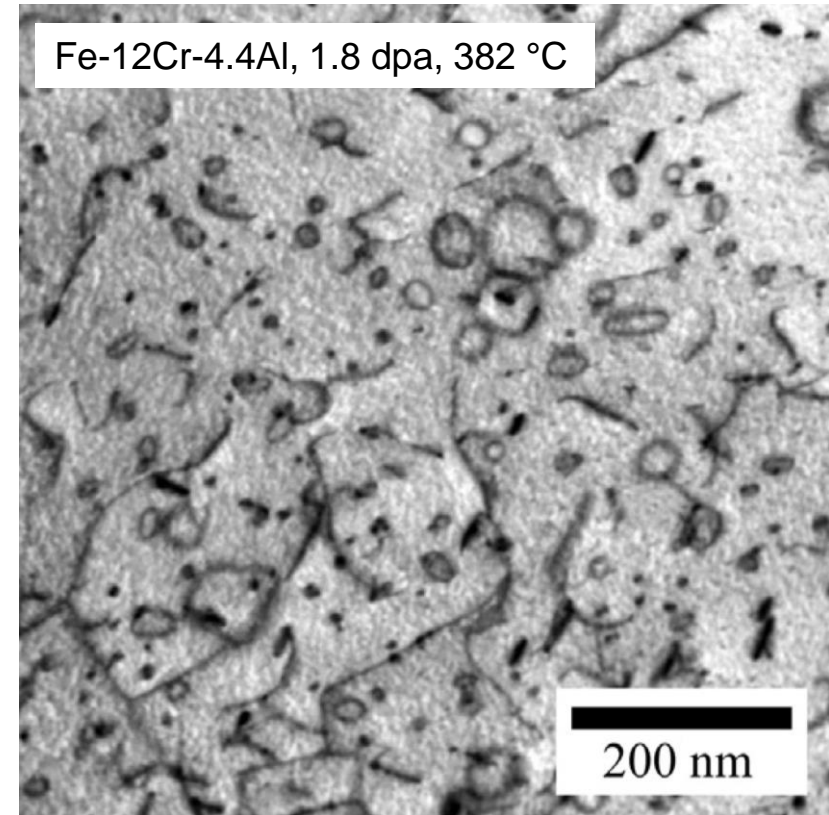
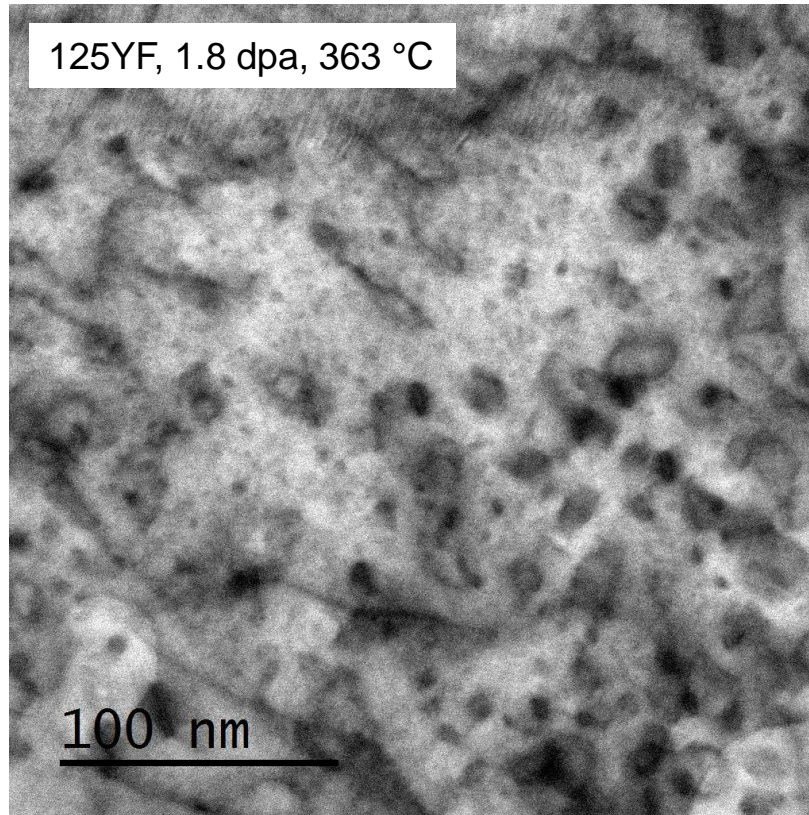
125YF Dislocation Loop Microstructures

- Low temp irradiation resulted in high density of small, mostly black-dot loop defects
- Medium temp irradiation yielded lower density of larger, more well defined loop structures
- No loop structures observed in high temp irradiation



Comparison to non-ODS Alloys

- Higher density of smaller loops observed in ODS variant
- Smaller grain size may also contribute to observed effect



Future Work

- APT analysis of ODS and α' microstructures
 - In-depth chemical analysis of precipitates
 - More insight into precipitate phase/chemistry/structure
- Correlation of microstructural data with change in mechanical properties (DBH or similar models)
- Similar studies on higher dose alloys, as well as on alloys containing ZrO_2 and TiO_2 nanoparticles

Summary & Conclusions

- Low-temperature irradiation has caused mild embrittlement, little change in mechanical properties in medium- and high-temperature irradiations
- EFTEM and SANS results suggest nanoparticle instability at low temperatures and coarsening at high temperatures
- Dislocation loops in ODS FeCrAl are much smaller than conventional alloys and a strong temperature dependence for loop size and density is observed
- Some evidence of α' precipitation is observed, but quantification of the distribution of this phase was not performed at this time.



ODS nanoparticles in FeCrAl alloys appear to be stable at LWR-relevant conditions, with marked improvements in radiation tolerance and mechanical strength over conventional alloys



Acknowledgements

- Primary funding provided by the U.S. Department of Energy (DOE), Office of Nuclear Energy, Advanced Fuel Campaign of the Fuel Cycle R&D Program and the U.S. DOE's Office of Science, Fusion Energy Sciences
- Use of CG-2 General Purpose SANS beamline at ORNL's HFIR facility sponsored by the U.S. DOE, Scientific User Facilities Division, Office of Basic Energy Sciences
- This research was performed, in part, using instrumentation (FEI Talos F200X TEM) provided by the Department of Energy, Office of Nuclear Energy, Fuel Cycle R&D Program, and the Nuclear Science User Facilities.



Thank you for your attention.
Questions?

Characterization techniques for nanoparticles

	Advantages	Disadvantages
Energy Filtered TEM (EFTEM)	<ul style="list-style-type: none">• Reveals microstructural heterogeneities• Quick/easy to perform• Direct microstructure observation	<ul style="list-style-type: none">• Poor signal to noise ratio; can limit resolution• Moderate volume analyzed• Highly dependent on sample quality• Limited composition information
Small Angle Neutron Scattering (SANS)	<ul style="list-style-type: none">• Large sampling volume; excellent counting statistics• Limited to no sample prep• Quick/easy to perform• Composition can be inferred (magnetic SANS only)	<ul style="list-style-type: none">• Indirect microstructure observation• No microstructural relationships (i.e. assumes homogenous distributions)• Requires bulk sample; increased radioactivity
Atom Probe Tomography (APT)	<ul style="list-style-type: none">• Composition information readily available• Excellent spatial resolution• Direct microstructure observation	<ul style="list-style-type: none">• Small sample volume analyzed• Dependent on sample quality• Data interpretation can be convoluted; aberration effects• Time intensive

Motivation: Accident Tolerant Fuel Forms

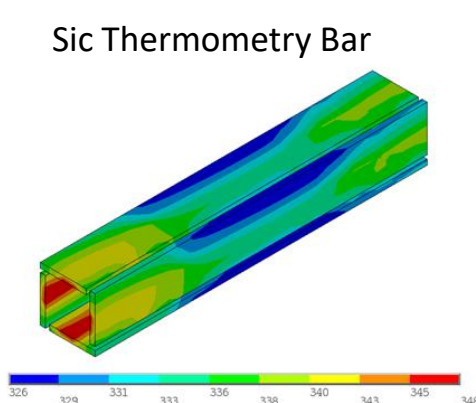
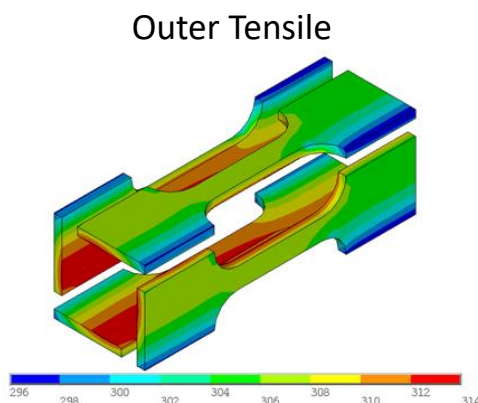
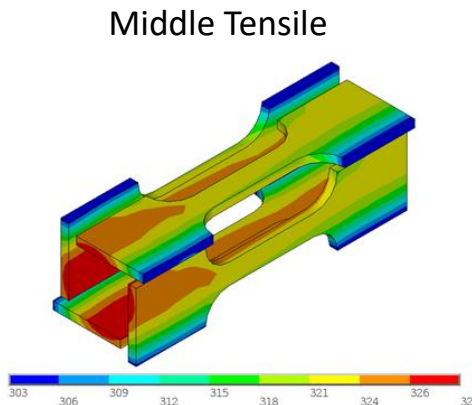
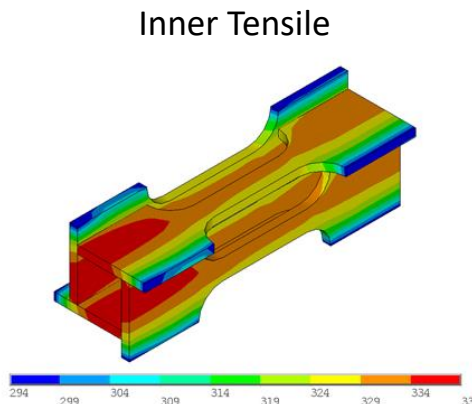
- Fukushima accident has demonstrated that Zircaloy cladding is detrimental in Loss of Coolant Accident (LOCA) scenarios
 - Exothermic oxidation reaction with H_2O produces H_2 gas
- DOE has funded development of accident-tolerant fuel (ATF) and fuel claddings
 - **Fe-Cr-Al Claddings**
 - **SiC/SiC Composite Claddings**
 - **SiC/Cr/MAX-phase Coatings for Zr**
 - **High-density/high-conductivity fuels (UN, U_3Si_2)**



Full SANS/EFTEM Comparison

Specimen ID	Irradiation Temp. (°C)	Number Density (x10 ²³ #/m ³)			Volume Fraction (%)			Mean Radius (nm)		
		SANS MD	SANS Monte Carlo	EFTEM	SANS MD	SANS Monte Carlo	EFTEM	SANS MD	SANS Monte Carlo	EFTEM
OD34	-	2.14±0.82	2.78±0.87	-	1.07±0.40	1.24±0.35	-	2.3±0.1	2.2±0.1 (unimodal)	-
OD01	195	5.02±2.80	1.54±0.54	1.04±0.24	0.96±0.45	1.01±0.33	0.43±0.28	1.7±0.2	2.5±0.1 (bimodal)	1.03±0.87
OD03	363	2.09±0.68	1.97±0.60	0.94±0.14	1.12±0.36	1.14±0.32	0.43±0.26	2.3±0.1	2.4±0.1 (unimodal)	1.27±0.90
OD06	559	1.39±0.80	1.89±0.61	0.49±0.34	0.72±0.41	1.24±0.37	1.56±1.93	2.3±0.1	2.5±0.1 (unimodal)	1.40±1.61

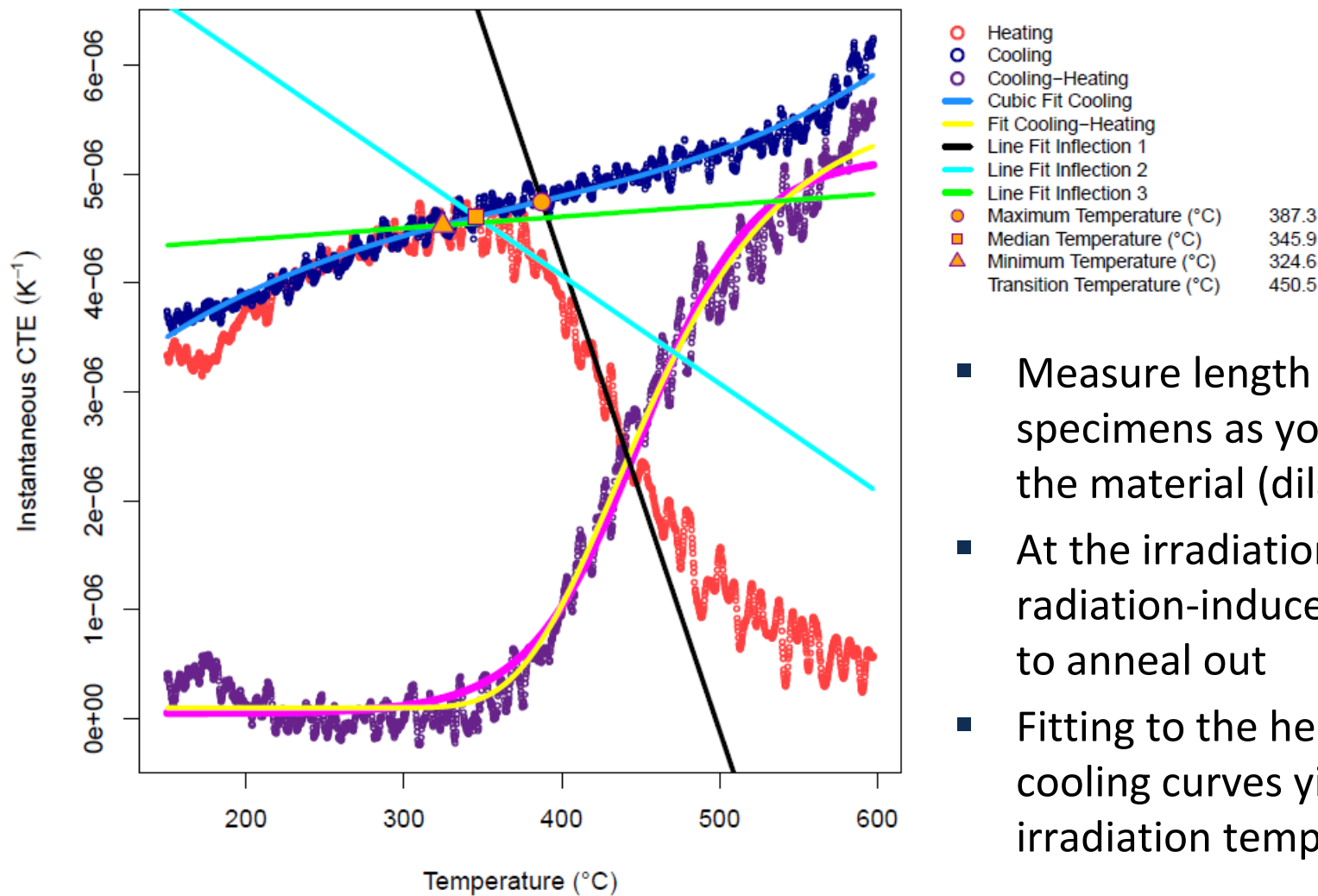
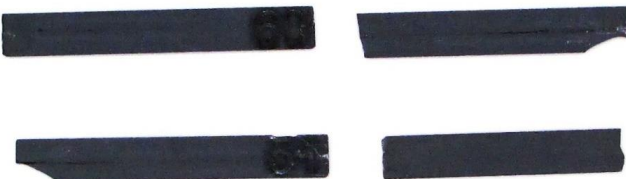
Irradiation Temperature Analysis



- Some thermal gradient expected in uninstrumented neutron-irradiation experiments
- Finite element analysis performed using ANSYS Workbench software using known HFIR heat generation rate and convection parameters
- Average temperatures within ~ 20 °C

Specimen	Specimen Temp (°C) Average (Min-Max)
Inner Tensile	328 (294-339)
Middle Tensile	321 (303-329)
Outer Tensile	307 (296-314)
SiC Thermometry	336 (328-344)

SiC Thermometry



- Measure length change of specimens as you heat and cool the material (dilatometry)
- At the irradiation temperature, radiation-induced defects begin to anneal out
- Fitting to the heating and cooling curves yields the irradiation temp

Fe-Cr-Al Alloy Development Campaign

Phase 1: Feasibility

Phase 2: Development/Qualification

Phase 3:

Commercialization

2012

2013

2014

2015

2016

2017

2018

2019

2020

2021

LTA/LTR Ready

Fabrication:

- Welding
- Tube fabrication
- TMT/Microstructure

Environment effects:

- Steam Oxidation resistance
- Environmental corrosion
- Thermal effects
- Radiation effects

Mechanical properties:

- Burst testing
- RT tensile properties
- High temperature tensile prop.
- Creep

Gen I Alloys:
Effect of Major Alloying Elements

Primary assessments:

- Impact on economics
- Impact on fuel cycle
- Impact on operations
- Impact on safety envelope

LOCA/Furnace Tests:

- Surrogate fuel tests
- Fueled and irradiated tests

Steady State Tests:

- Fuel-cladding chemical interaction
- In-pile creep/swelling
- Instrumented water loop

Baseline Assessments:

- Fabrication
- Environmental effects
- Mechanical properties

Gen II Alloys:

Effect of Minor Alloying Elements + More complex experimentation

Baseline Assessments:

- Fabrication
- Environ. effects
- Mechanical prop.

Steady State Tests

Nuclear Grade Alloy(s):
Optimized properties for normal and off-normal conditions

Re-assessments:

- Economics
- Fuel cycle
- Operation
- Safety envelope

Transient Irradiation Tests:

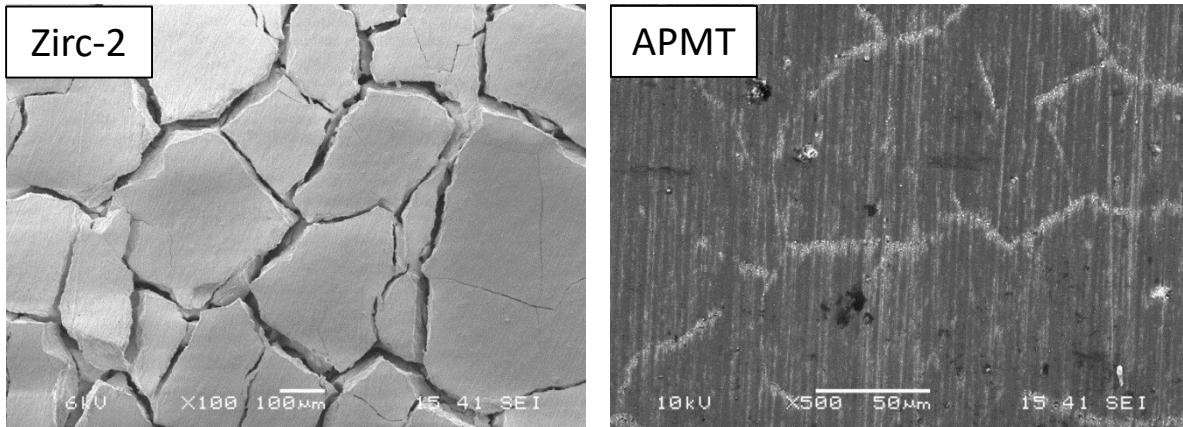
- Fuel meltdown
- Metal-water reactions

Fuel Performance Code

Fuel Safety Basis

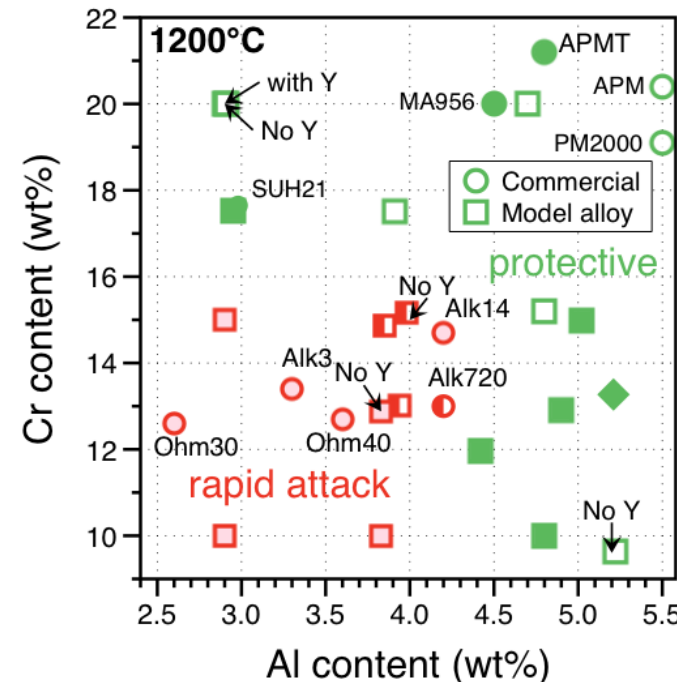
Fe-Cr-Al alloys for Nuclear Systems

- Why is Fe-Cr-Al attractive as a LWR cladding material?
 - Exceptional high temperature oxidation resistance due to formation of passivating Al_2O_3 (up to 1200-1475 °C)
 - High strength, with potential for oxide-dispersion strengthened variants
 - Low swelling rates in irradiation environments
 - Potential for near-term deployment



24 hrs, 1000 °C, 100% Steam

Images courtesy of Raul Rebak, GE Global Research

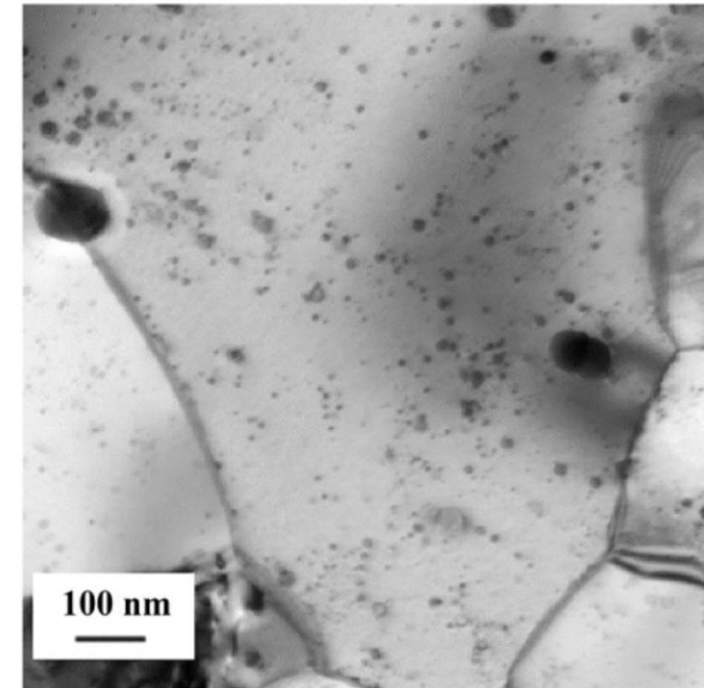
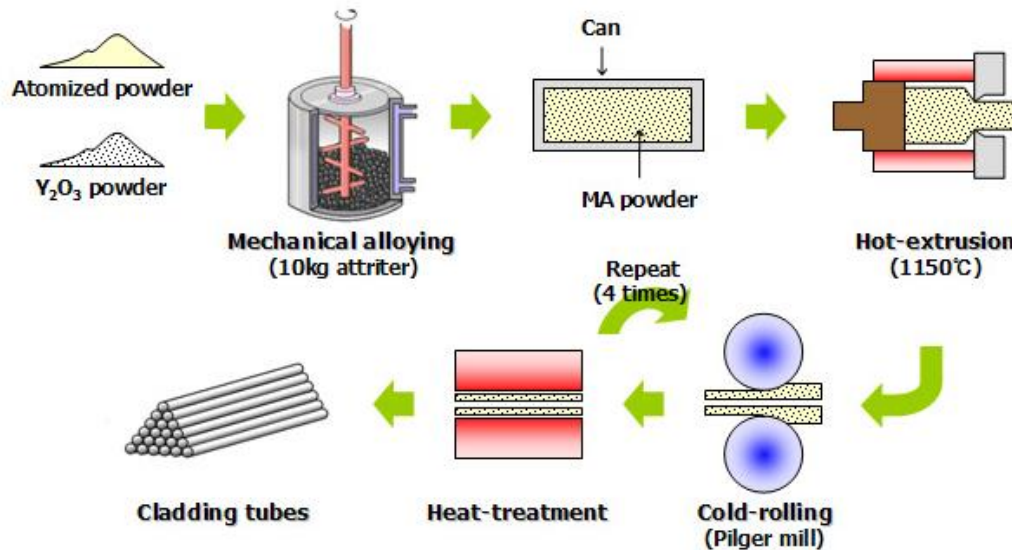


High temperature oxidation of model Fe-Cr-Al alloys exposed to steam at 1200 °C [1]

[1] Pint, B. A., Unocic, K. A., & Terrani, K. A. (2015). Effect of steam on high temperature oxidation behaviour of alumina-forming alloys. *Materials at High Temperatures*, 32(1-2), 28–35.

ODS FeCrAl Motivation

- Oxide dispersion-strengthened FeCrAl variants seek to increase alloy strength and creep resistance
- Have the added benefit of introducing a high density of interfaces that serve as sinks for point defects
 - Results in enhanced radiation tolerance

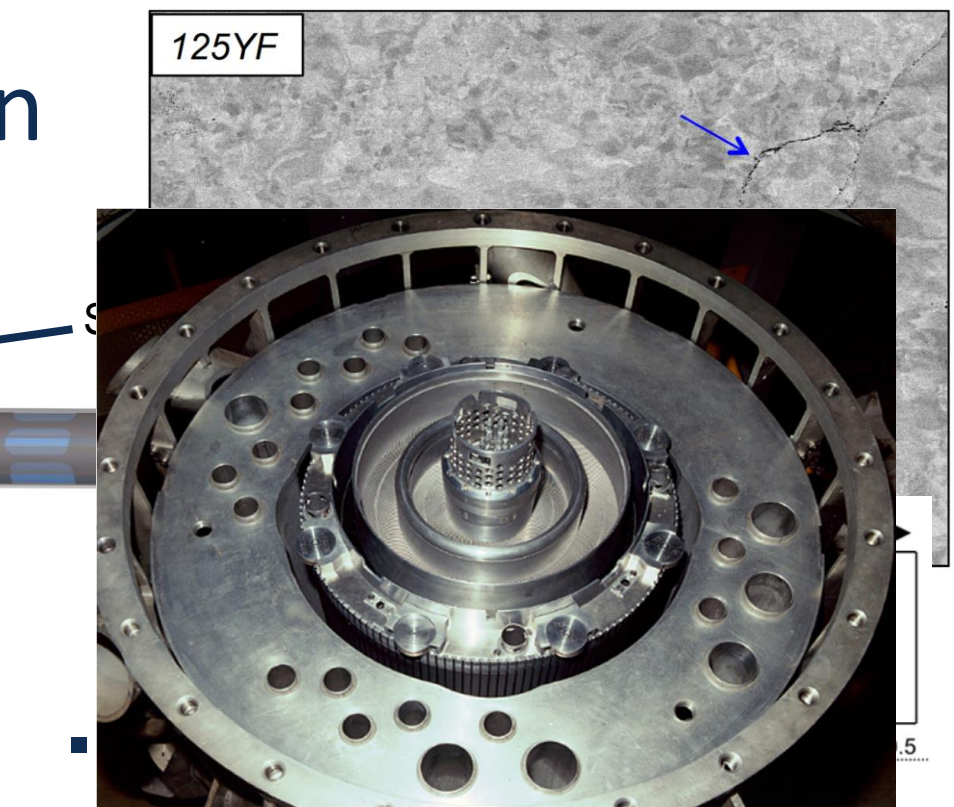


Microstructure of ODS Fe-14Cr-1W-0.4Ti following 30 min anneal at 1150 °C

Experimental Design



40 hrs, degassed for 24 hrs at 300 °C,
and extruded at 950 °C.¹



alumina stringers apparent

Capsule ID	Exposure Time (hrs)	Neutron Flux (n/cm ² s) E > 0.1 MeV	Neutron Fluence (n/cm ²) E > 0.1 MeV	Dose Rate (dpa/s)	Dose (dpa)	Irradiation Temperature (°C)
FCAT-01	590	1.10×10^{15}	2.17×10^{21}	9.8×10^{-7}	1.9	194.5 ± 37.9
FCAT-02	590	1.04×10^{15}	2.17×10^{21}	9.3×10^{-7}	1.8	363.6 ± 23.1
FCAT-03	590	1.10×10^{15}	2.17×10^{21}	9.8×10^{-7}	1.9	559.4 ± 28.1

FCAY and FCAT Rabbits

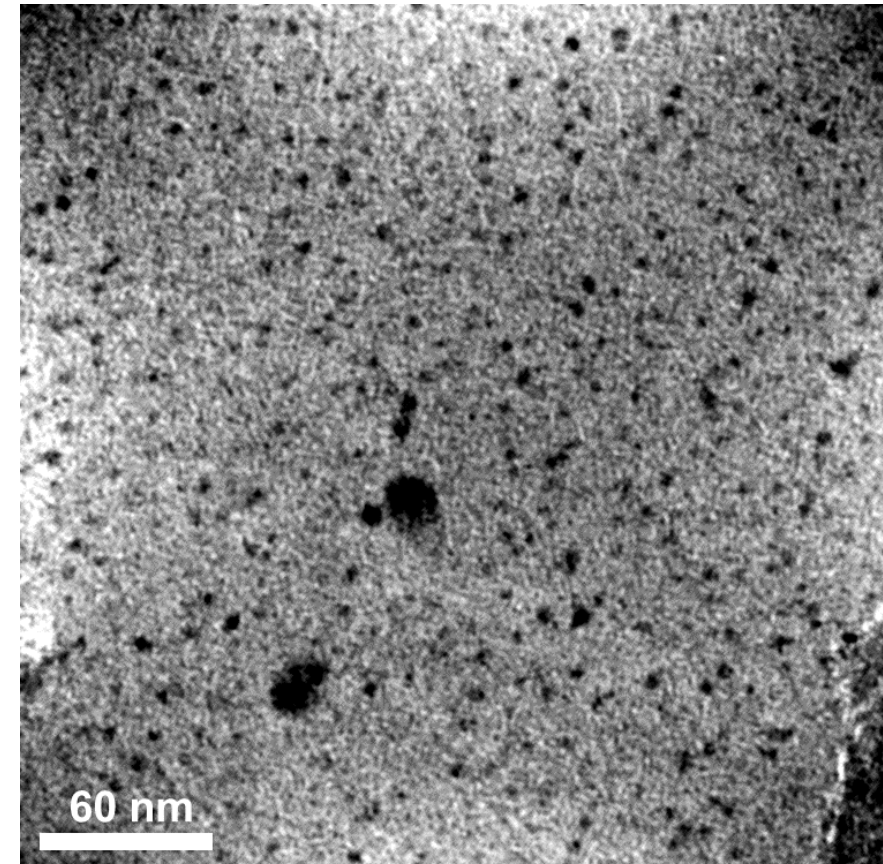
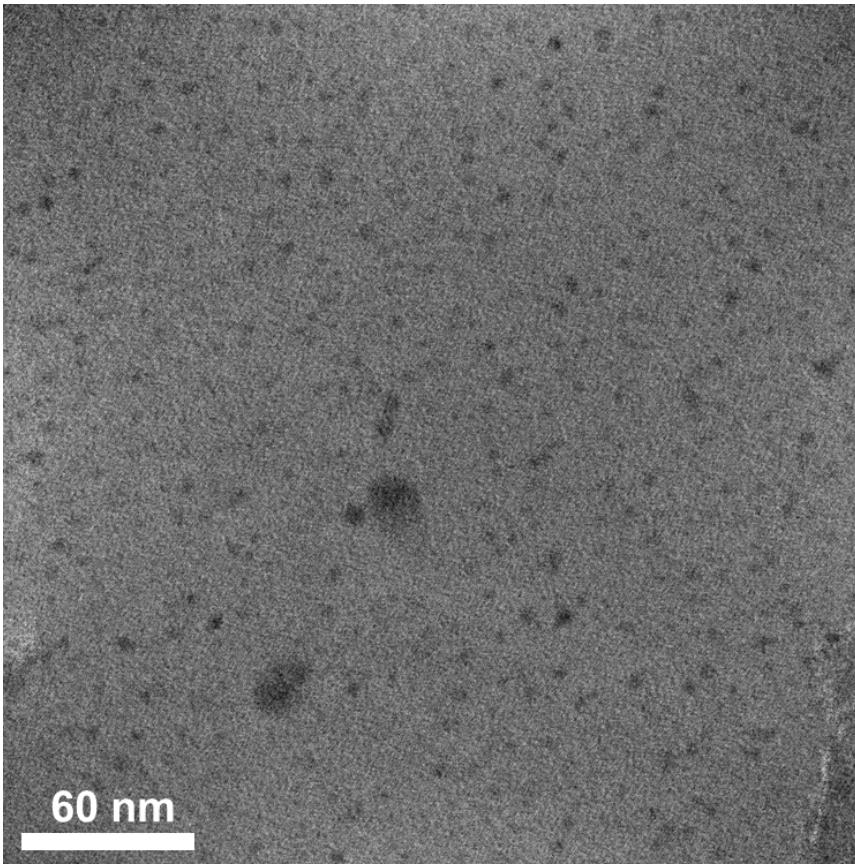
Alloys studied:

1. Model alloys (M): F1C5AY, B125Y, B154Y-2, B183Y-2
2. Engineering grade alloys (E): C06M, C35M, C36M, C37M, C35MN, C35M10TC
3. Commercial alloys (C): Kanthal APMT™, and Alkrothal 720
4. ODS Alloys (O): 125YF



125YF Oxide Microstructures

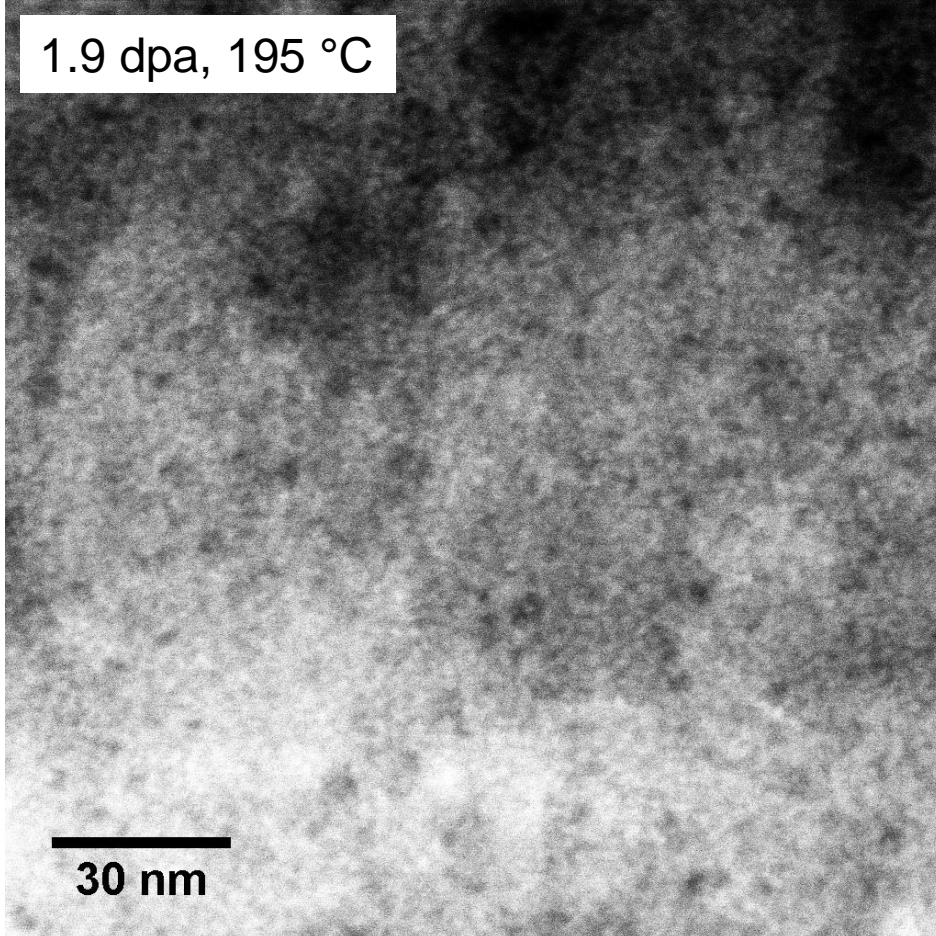
- EFTEM Fe-M jump-ratio images to look at ODS particles
- B/C correction + mean image filter to enhance contrast
- No evidence of α' phase in Cr-M jump ratio images



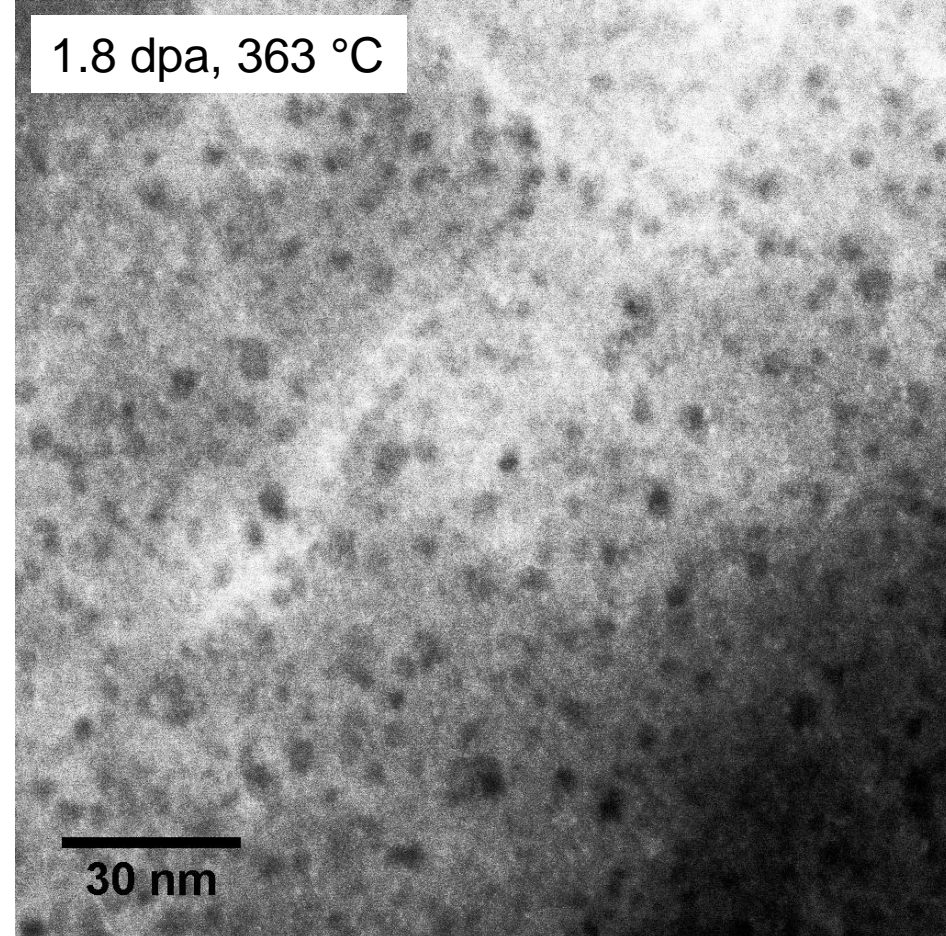
125YF Oxide Microstructures

- Yttria/alumina precipitates decorating some GBs, some larger precipitates in the matrix

1.9 dpa, 195 °C



1.8 dpa, 363 °C



30 nm

30 nm